Chemical Science

ROYAL SOCIETY OF CHEMISTRY

EDGE ARTICLE

View Article Online
View Journal | View Issue

Cite this: *Chem. Sci.*, 2020, **11**, 6701

All publication charges for this article have been paid for by the Royal Society of Chemistry

Received 22nd April 2020
Accepted 30th May 2020

DOI: 10.1039/d0sc02286a

rsc.li/chemical-science

Single-atom replacement as a general approach towards visible-light/near-infrared heavy-atom-free photosensitizers for photodynamic therapy†

Juan Tang,‡[a] Lushun Wang,‡[a] Axel Loredo,[a] Carson Cole[a] and Han Xiao *[abc]

Photodynamic therapy has become an emerging strategy for the treatment of cancer. This technology relies on the development of photosensitizers (PSs) that convert molecular oxygen to cytotoxic reactive oxygen species upon exposure to light. In this study, we have developed a facile and general strategy for obtaining visible light/near-infrared-absorbing PSs by performing a simple sulfur-for-oxygen replacement within existing fluorophores. Thionation of carbonyl groups within existing fluorophore cores leads to an improvement of the singlet oxygen quantum yield and molar absorption coefficient at longer wavelengths (deep to 600–800 nm). Additionally, these thio-based PSs lack dark cytotoxicity but exhibit significant phototoxicity against monolayer cancer cells and 3D multicellular tumor spheroids with IC_{50} in the micromolar range. To achieve tumor-specific delivery, we have conjugated these thio-based PSs to an antibody and demonstrated their tumor-specific therapeutic activity.

Introduction

Photodynamic therapy (PDT) is a photochemistry-based treatment that combines two nontoxic modalities, photosensitizers (PSs) and light, to produce reactive oxygen species that are toxic to targeted cells and tissues.[1–5] Over the past three decades, PDT has received increasing attention in the context of cancer treatment due to its high degree of spatiotemporal selectivity and minimal invasiveness, properties that are superior to those seen with traditional chemotherapy and radiotherapy.[6–12] Central to PDT is the development of PSs. Upon photoexcitation, the PS is excited to a singlet state and then undergoes intersystem crossing (ISC) to a longer-lived triplet state that triggers the photodynamic therapeutic effect *via* generation of cytotoxic radical ions or singlet oxygen species.[13–19] To enhance ISC efficiency, heavy atoms have been incorporated into PS structures. These compounds, however, are not only difficult to synthesize but are often costly and suffer from strong cytotoxicity in the absence of irradiation.[20–23] Therefore, it is desirable for PDT applications to design heavy-atom-free PSs that exhibit high singlet oxygen quantum yield, low cytotoxicity in the dark, and a high molar absorption coefficient at long wavelengths (600–800 nm) that can penetrate deeply into tissues.[24–31]

Thiobases (*e.g.*, thiopurines, thioguanine, and others) have received much attention for use in photodynamic therapy and photo-crosslinking applications.[32–36] Because thiocarbonyl compounds exhibit a stronger spin–orbit coupling effect between singlet and triplet states than corresponding carbonyl compounds [spin–orbit coupling (SOC) constant of 397 cm^{-1} for S *vs.* 152 cm^{-1} for O], they exhibit a higher probability to undergo ISC.[37,38] Thiocarbonyl compounds, therefore, generate efficient populations of long-lived, active triplet excited states capable of sensitizing molecular oxygen and yielding highly unstable reactive oxygen species (ROS) upon irradiation. Nevertheless, the requirement for relatively high doses and longer UVA irradiation times has dramatically limited applications of these thiobases.[39–41] In 2019, we developed a general approach for preparing thio-based fluorophores across a broad emission range (294–626 nm) for use in biological imaging.[42] We found that these thio-based fluorophores exhibited significant bathochromic shifts in absorption maxima (more than 170 nm), as well as enhanced extinction coefficients compared to corresponding carbonyl compounds. These properties improve the tissue penetration and light absorbance efficiency, respectively, of the thio-based compounds. More importantly, upon excitation with visible light, singlet oxygen species are generated by these thio-based fluorophores, indicating the likelihood that they can serve as PSs for PDT applications.[42] During our preparation of this manuscript, Nguyen *et al.* reported the preparation of thio-based naphthalimide dyes and their utility for photodynamic studies,[43] reinforcing the potential utility of thio-based fluorophores for PDT. Taking all of the above into

[a]*Department of Chemistry, Rice University, 6100 Main Street, Houston, Texas, 77005, USA. E-mail: han.xiao@rice.edu*

[b]*Department of Biosciences, Rice University, 6100 Main Street, Houston, Texas, 77005, USA*

[c]*Department of Bioengineering, Rice University, 6100 Main Street, Houston, Texas, 77005, USA*

† Electronic supplementary information (ESI) available. See DOI: 10.1039/d0sc02286a

‡ These authors contributed equally.

account, we envision that thiocarbonyl substitution within common biocompatible fluorophores of any wavelength represents a general approach toward yielding heavy-atom-free PSs with excellent potential for use in PDT (Fig. 1).

Herein, we report a new class of thio-based and heavy-atom-free PSs. These compounds exhibit near unit yields of singlet oxygen, high light absorption efficiency, and tunable absorption wavelengths even in the near-infrared (NIR) region. We demonstrate that the replacement of a single oxygen atom with sulfur in common fluorophores can lead to a dramatic generation of singlet oxygen upon excitation with visible or NIR light within their absorption range (365 nm–760 nm). Moreover, these compounds exhibit good photodynamic therapeutic efficacy against monolayer cancer cells and 3D multicellular tumor spheroids. As examples of tumor-targeting applications, we demonstrate the tumor-specific photoimmunotherapy by conjugating a thio-based PS to trastuzumab, a monoclonal antibody directed against human epidermal growth factor receptor 2 (HER2). This conjugate exhibits robust cytotoxicity against HER2-positive cell lines, but almost no activity against HER2-negative cells, suggesting its great promise for the selective treatment of HER2 positive breast cancer.

Results and discussion

Synthesis and characterization of thio-based photosensitizers

To test whether a single sulfur-for-oxygen atom replacement within common fluorophore scaffolds represents a general approach to preparing PSs, we synthesized several thio-based dyes, including thio-acridone (SACD), thio-coumarin (SCou), thio-4-dimethylaminophthalimide (SDMAP), thio-4-dimethylamino-1,8-naphthalimide (SDMN), thio-4-dimethylaminonaphthalimide (SDMNP), and thio-based Nile Red (SNile Red) (Fig. 1). Treatment of the oxo forms of fluorophores with Lawesson's reagent in refluxing toluene produced the desired thio-based fluorophores with yields ranging from 20–80% (ESI†). Structures of the resulting compounds were fully verified and characterized by high-resolution electrospray ionization mass (HR-ESI-MS) spectrometry, ^{1}H NMR, ^{13}C NMR, and infrared spectroscopy (ESI†).

We characterized the photophysical properties of these thiofluorophores and their oxygen congeners using UV-vis and fluorescence spectroscopies (Table 1 and Fig. S1 and S2†). Generally, the thiocarbonyl fluorophores exhibited distinct bathochromic shifts (up to 173 nm shift) and larger extinction coefficients at their absorption maxima compared to the carbonyl analogs. Thiocarbonyl group substitution within carbonyl fluorophores also leads to significant fluorescence loss (lowering the fluorescence quantum yields almost to zero), as reported previously.[42] As emitting fluorescence and ISC are two competitive processes, we supposed the dramatic fluorescence quenching indicates the possibility that thionation induces an efficient ISC transformation from singlet excited state to the triplet state. To test this hypothesis, we measured the relative singlet oxygen quantum yields of thio-based fluorophores. 1,3-Diphenylisobenzofuran (DPBF) was used as the singlet oxygen detection reagent,[44] while methylene blue (MB) (Φ_Δ = 0.57 in DCM)[46] or Ru(bpy)$_3^{2+}$ (Φ_Δ = 0.73 in MeOH)[45] were used as references. The singlet oxygen quantum yields and other photophysical data are compiled in Table 1 and Fig. S3.† Each of the

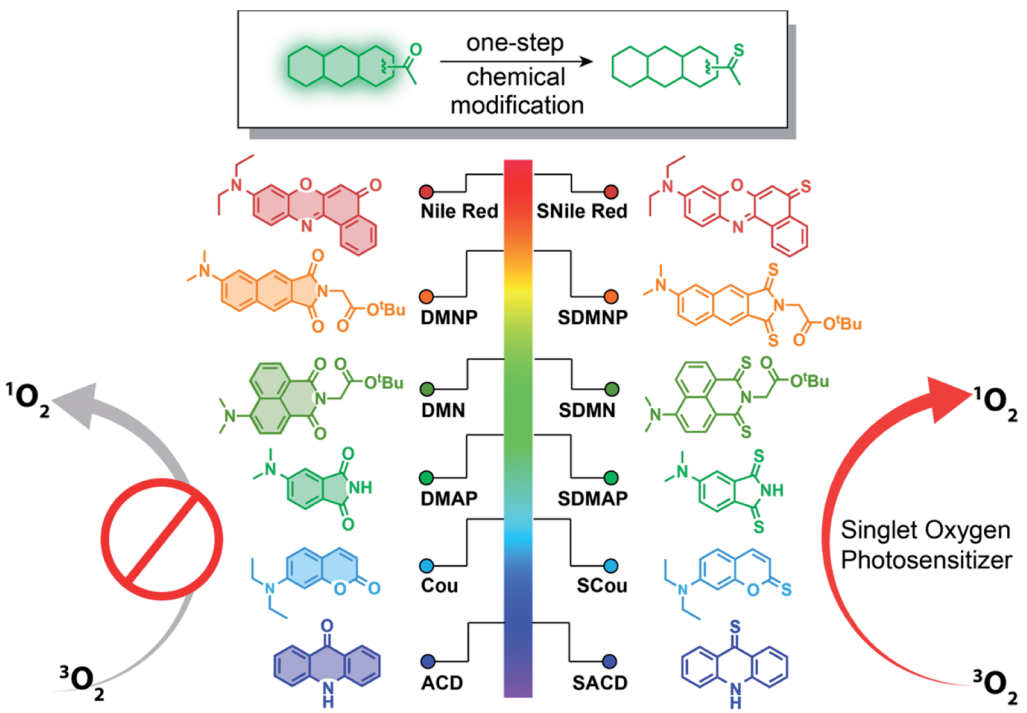

Fig. 1 Design of thio-based PSs. Thiocarbonyl substitution at the carbonyl group of a variety of fluorophores can dramatically enhance their abilities to generate ROS. Illustrated are structures of the starting (left) and thio-based fluorophores (right) described in this study.

Table 1 Photophysical and photosensitizing data of thio-based photosensitizers and their oxygen congeners

PSs[a]	λ_{abs}[a] (nm)	$\varepsilon^{a,b}$ ($\times 10^4$ M^{-1} cm^{-1})	λ_{em}[a] (nm)	Φ_f[c]	Φ_Δ[d]
Cou	261, 378	0.95, 2.82	445	0.71	—
SCou	273, 476	1.43, 2.79	453	<0.001	0.64
ACD	361, 379, 398	0.50, 1.0, 1.16	406, 428, 455	0.64	—
SACD	430, 456, 485	0.52, 1.50, 2.55	409, 427, 463	<0.001	~1
DMAP	262, 322, 390	0.56, 0.28, 0.20	505	0.09	—
SDMAP	326, 390, 563	3.02, 2.78, 1.02	447	<0.001	~1
DMN	266, 279, 431	1.50, 1.48, 1.08	521	0.007	—
SDMN	377, 420, 604	0.80, 0.45, 1.48	—	<0.001	~1
DMNP	281, 384	2.74, 1.71	551	0.16	—
SDMNP	264, 388, 586	1.77, 1.32, 0.38	435	<0.001	0.81
Nile Red	315, 556	0.92, 4.17	626	0.46	—
SNile Red	298, 368, 652	1.73, 0.97, 4.47	616	<0.001	0.36

[a] Compounds were dissolved in DMSO (50 μM). [b] Extinction coefficients. [c] Fluorescence quantum yields were measured using rhodamine B in ethanol, quinine sulfate in 0.5 M H_2SO_4 as the reference or fluorescein in 0.1 M NaOH. [d] Singlet oxygen quantum yields were determined with respect to $Ru(bpy)_3^{2+}$ for SCou and SACD (Φ_Δ = 0.73 in MeOH)[45] and Methylene Blue for SDMAP, SDMN, SDMNP and SNile Red (Φ_Δ (MB) = 0.57 in DCM).[46] (—), not observed.

thiocarbonyl fluorophores exhibited distinct singlet oxygen quantum yields (Φ_Δ, from 0.36 to 1.00), while no singlet oxygen generation was detected for the oxygen congeners. To probe the photosensitizing mechanism induced by a single sulfur-for-oxygen atom replacement, we used theoretical calculations to evaluate the spin–orbital coupling (SOC) constants for the optimized structures of the carbonyl and thiocarbonyl compounds. Taking DMNP and SDMNP as examples, we found that the SOC constants from S1 state to T1 state were 0.18892 cm^{-1} and 71.81998 cm^{-1} for DMNP and SDMNP, respectively (Table S1†). SOC is therefore significantly enhanced by replacing the carbonyl moiety with a thiocarbonyl moiety, suggesting that, compared to oxygen congeners, thiocarbonyl compounds have a higher probability for ISC and enhanced sensitization toward the ground-state triplet oxygen. Given the significant bathochromic shifts of thio-based PSs in absorption maxima and their enhanced extinction coefficients (Table 1), properties that enhance light penetration depth and light absorbance efficiency, respectively, we consider thiocarbonyl fluorophores to be outstanding PS candidates for PDT.

Applications of thio-based photosensitizers in photodynamic therapy

Since PSs are widely used for PDT, we initially evaluated the activity of our thio-based PSs by using a CCK-8 assay to quantify numbers of viable HeLa cells (human cervical cancer) following photodynamic treatment. Taking into account the poor solubility of SDMAP, we used the more water-soluble SDMAP-Halo[42] for this cellular work. Cells were incubated with PSs (3 μM) for 2 hours, irradiated under light (400–700 nm, 0.4 μW cm^{-2}) for 20 minutes, and then cultured in the dark for another 24 hours. The 20 minutes irradiation was omitted to establish control conditions. As shown in Fig. 2A, while almost none of the thio-based PSs are effective in the absence of light, following irradiation they each exhibit a different level of potency in reducing HeLa cell number (SDMNP ≈ SDMN > SACD > SNile Red > SDMAP-Halo > SCou). Since these fluorophores have different core structures, leading to differences in light absorption efficiency, cellular permeability, cellular accumulation and subcellular distribution, it is understandable there is no obvious correlation between the singlet oxygen quantum yield and the observed level of photodynamic activity against HeLa cells. Additionally, we investigated the activity of these thio-based PSs following irradiation with light in the red or NIR region, a critical issue for increasing the depth of light penetration in tissues. Both SDMNP (with strong absorption at 500–700 nm) and SNile Red (with strong absorption at 550–750 nm) exhibited robust ability to reduce HeLa cell number, with IC_{50} (the half-maximal inhibitory concentration) of 0.26 ± 1.09 μM for SDMNP induced by 600–630 nm light and 2.19 ± 1.45 μM for SNile Red induced by 730 nm light (Fig. 2B and S4†). It is worth noting that most investigated anticancer agents working well to monolayer cancer cells would however fail during translation to *in vivo* models, which is partially due to mass transport limitations from extracellular barriers.[47–49] Large 3D multicellular tumor spheroids (MCTS) (~400–500 μm diameter) display a closely packed cell arrangement with a reduced diffusion rate of drugs and oxygen through the spheroids, which is comparable to the *in vivo* solid tumor models. Thus, MCTS has been widely used for cancer research by mimicking growth, shape and structural features of *in vivo* tumor.[49–53] Therefore, we investigated the photocytotoxic effect of SDMNP towards HeLa MCTS with diameters of *ca.* 500 nm (Fig. S5†). The photodynamic killing effect was determined by measurement of the adenosine triphosphate (ATP) concentration in the tumor spheroids using CellTiter-Glo 3D Cell Viability kit (Promega). While SDMNP showed no toxicity in dark to MCTS, it showed a significant effect on the cell viability under light irradiation (400–700 nm, 0.4 μW cm^{-2}), giving IC_{50} value of 1.58 ± 1.06 μM (Fig. S6†). It was slightly higher than that in the 2D monolayer cancer (0.65 ± 0.77 μM), probably due to the limited penetration of light into the MCTS and the reduced oxygen level in MCTS. To further demonstrate the photodynamic therapeutic effect of SDMNP to MCTS, LIVE/DEAD co-staining kit was applied to

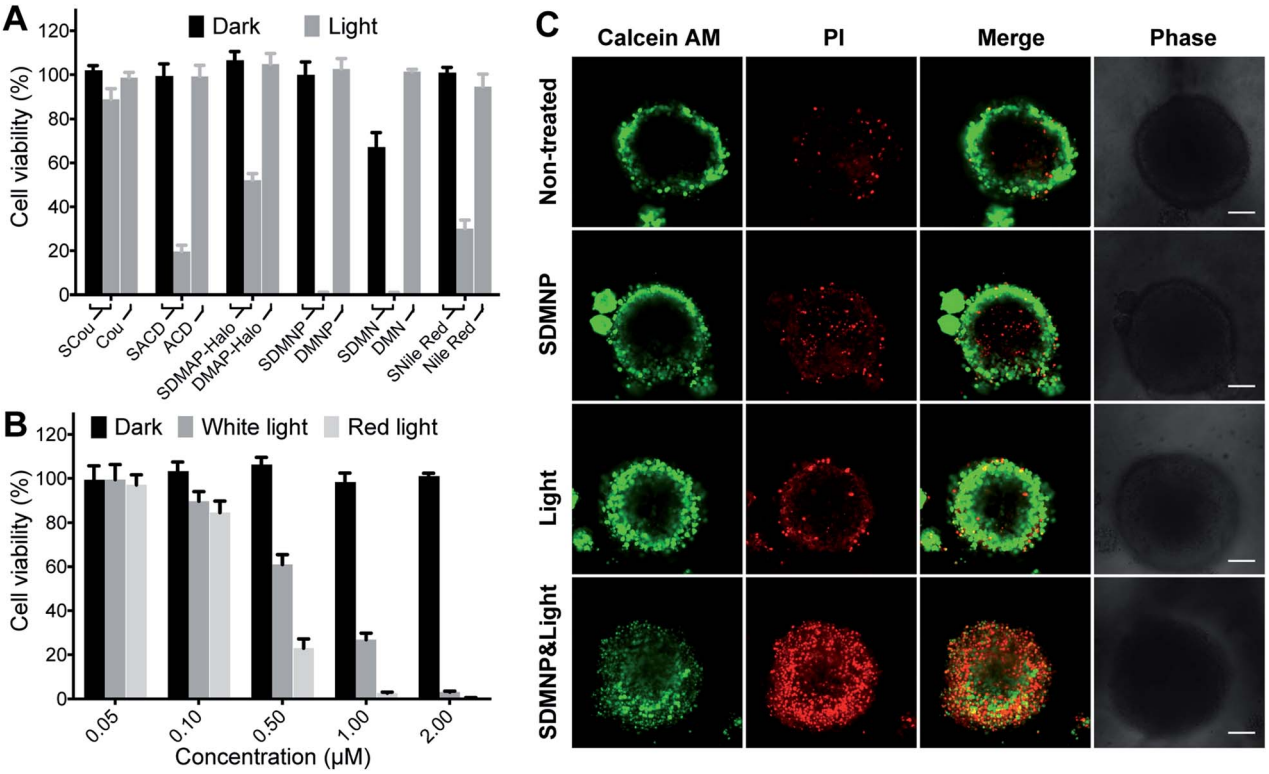

Fig. 2 (A) Cell viability of HeLa cells after treatment with 3 μM PSs. (B) Cell viability of HeLa cells after treatment with different concentrations of SDMNP in the presence and absence of white light (400–700 nm) or red light (600–630 nm). (C) Confocal images of HeLa MCTS loaded with Calcein AM/PI. Scale bar: 100 μm.

different groups of HeLa MCTS, in which Calcein AM and propidium iodide (PI) were used to label living and dead cells, respectively. As shown in Fig. 2C, MCTS treated with both SDMNP and light showed strong red fluorescence and weak green fluorescence, indicating MCTS was mostly eradicated. In contrast, MCTS without any treatment or treated with only SDMNP or light presented strong green fluorescence with very weak red fluorescence, suggesting the intact MCTS. Overall, these results indicate the potential value of thiocarbonyl fluorophores as PSs for PDT application.

Mechanistic aspects of SDMNP action in photodynamic therapy

Following up on these preliminary indications that thio-based PSs might induce photocytotoxicity in cancer cells, we investigated in more detail the mechanism underlying the photodynamic activity of SDMNP. Initially, we used a confocal laser scanning microscope (CLSM) to visually monitor the photodynamic effect of SDMNP on HeLa cells. After incubation with SDMNP for 2 h, HeLa cells were irradiated with the CLSM 405 nm laser (100%, 20 mW). As shown in Fig. 3A, this treatment produced obvious signs of acute cytotoxicity, reflected by cellular swelling and membrane bleb formation.[1–5] Untreated control cells exhibited no changes in morphology following the irradiation (Fig. 3A). To further explore the apparent photocytotoxicity induced by SDMNP in HeLa cells, we used a LIVE/DEAD co-staining assay. As shown in Fig. 3B, irradiation in the presence of SDMNP caused dramatic cell death, as evidenced by substantially increased numbers of propidium iodide-positive cells and very few Calcein AM-positive cells. By contrast, no obvious evidence of cell death was observed in the three control groups (non-treated, SDMNP-treated only and light-irradiated only). These findings support our preliminary conclusion that the effects of irradiating SDMNP are due to the induction of cytotoxicity. The effects of long-term irradiation of SDMNP-treated HeLa cells were assessed using a CCK-8 assay. One day after light irradiation, SDMNP exerted a dose-dependent cytotoxic effect on HeLa cells with an IC_{50} value of 0.65 ± 0.77 μM (Fig. 2B). This is much lower than that of methylene blue (more than 10 μM) (Fig. S7†), a PS that has been used for the treatment of methemoglobinemia.[55] Additionally, we investigated the photocytotoxicity of SDMAP induced by light in the red region (600–630 nm), an important factor for increasing the depth of light penetration in tissues. As shown in Fig. 2B, SDMNP also exerted a robust cytotoxic effect after red light irradiation, with an IC_{50} toward HeLa cells of 0.26 ± 1.09 μM. These results confirm that SDMNP exhibits improved cytotoxicity under light irradiation and can, therefore, be exploited as an ideal PS for PDT application.

Light-induced ROS generation is an important causative factor in PDT-induced cell death. To examine the intracellular ROS generating ability of SDMNP, we used 2′,7′-dichlorodihydrofluorescein diacetate (H_2DCFDA) to probe the ROS level in HeLa cells.[56,57] As shown in Fig. 3C, cells treated with both

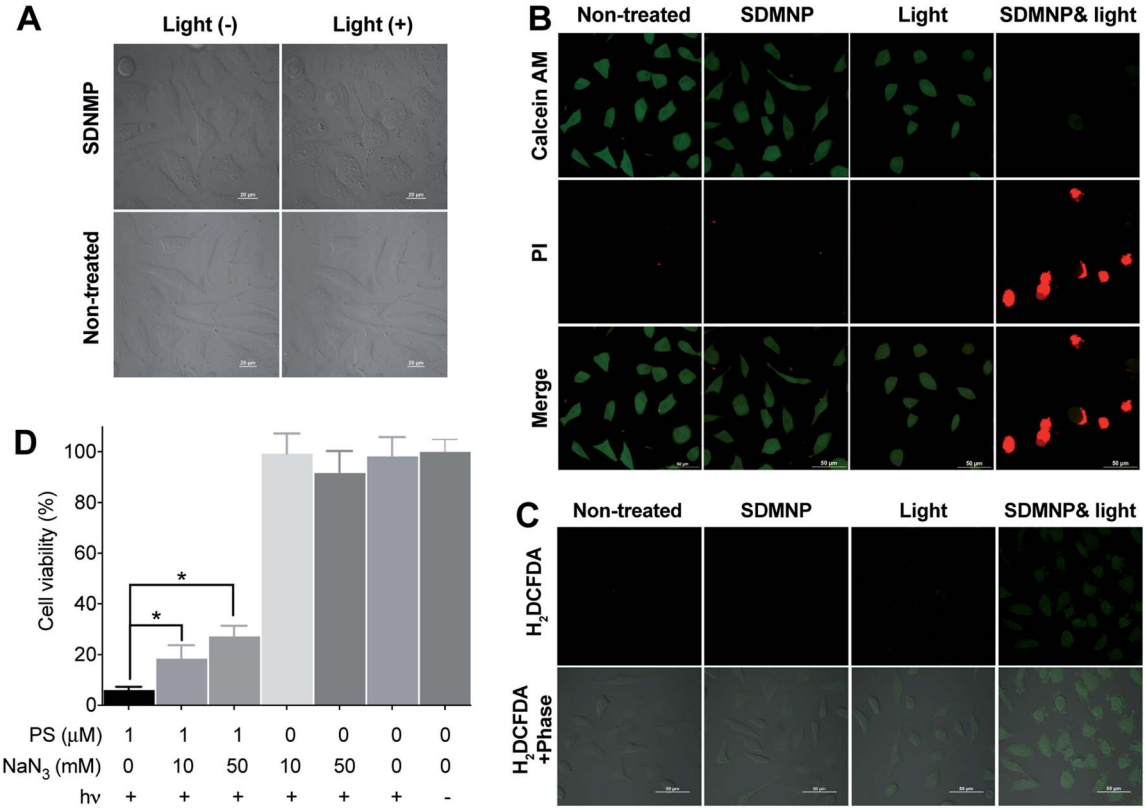

Fig. 3 (A) Cell morphological change in the presence or absence of 2 μM SDMNP before or after light irradiation (405 nm laser). Confocal images of HeLa cells loaded with (B) Calcein AM/PI or (C) H_2DCFDA. Scale bar: 50 μm. (D) Sodium azide (NaN_3) concentration-dependent effect of SDMNP on photocytotoxicity to HeLa cells. *P < 0.005.

SDMNP and irradiation exhibited stronger intracellular green fluorescence than cells in the three control groups (non-treated, SDMNP-treated only and light-irradiated only). This clear indication of intracellular ROS generation induced by SDMNP under irradiation is consistent with the cytotoxicity results. To clarify the role of singlet oxygen in the PDT, we incubated sodium azide (NaN_3, singlet oxygen quencher) with the cells during irradiation.[54,58,59] As shown in Fig. 3D, NaN_3 increased the percentage of surviving cells in a dose-dependent manner, suggesting that singlet oxygen is involved in the photocytotoxic effect.

Tumor-specific delivery of the photosensitizer

To achieve tumor-specific delivery of thio-based PSs, we conjugated SDMNP to trastuzumab (Tras), an antibody targeting the human epidermal growth factor receptor 2 (HER2). HER2, a transmembrane protein, is involved in the regulation of tumor differentiation and malignancy and has been recently identified as a clinically relevant target for the diagnosis and therapy of breast and gastric cancers.[60–62] Having identified SDMNP as an efficient thio-based PS for inducing cellular cytotoxicity upon light irradiation, we coupled thio-4-dimethylaminonaphthalimide-*N*-hydroxysuccinimide ester (SDMNP-NHS-Ester) to Tras to yield Tras-SDMNP conjugate (Fig. 4A). After an overnight reaction, excess linker was removed, and the extent of SDMNP-NHS-Ester modification of Tras was determined by ESI-MS. (Fig. S8†). First, we analyzed the photocytotoxicity of the small molecule, SDMNP-NHS-Ester, to HER2-positive SK-BR-3 cells and HER2-negative MDA-MB-468 cells. As shown in Fig. S9,† SDMNP-NHS-Ester alone did not show any selective killing against the HER2-expressing cell lines. Then the Tras-SDMNP conjugate was tested for photocytotoxicity and selectivity on SK-BR-3 cells and MDA-MB-468 cells. Cells were treated with the Tras-SDMNP conjugate for 2 h, followed by 20 min of irradiation (400–700 nm, 0.4 μW cm^{-2}). As shown in Fig. 4B, the viability of SK-BR-3 cells was significantly reduced by Tras-SDMNP in a dose-dependent manner, while little lysis was observed in HER2-negative MDA-MB-468 cells up to a concentration of 5 μM. The photoimmunotherapy effect on SK-BR-3 cells was also correlated with the time of irradiation. As the irradiation was extended from 0 min to 40 min, SK-BR-3 cell viability decreased from 102.1 ± 3.7% to 59.3 ± 3.1% (Fig. 4C). There is no difference in photocytotoxicity between 2 h and 24 h of incubation with Tras-SDMNP (Fig. S10†). In addition, Tras-SDMNP photocytotoxicity was totally blocked by co-incubation with 1 equiv. of wild type Tras (Fig. S11†), presumably due to competition for binding to the HER2 ligand. Overall, these results demonstrate that the Tras-SDMNP conjugate is able to induce cell cytotoxicity in a tumor- and light-dependent manner.

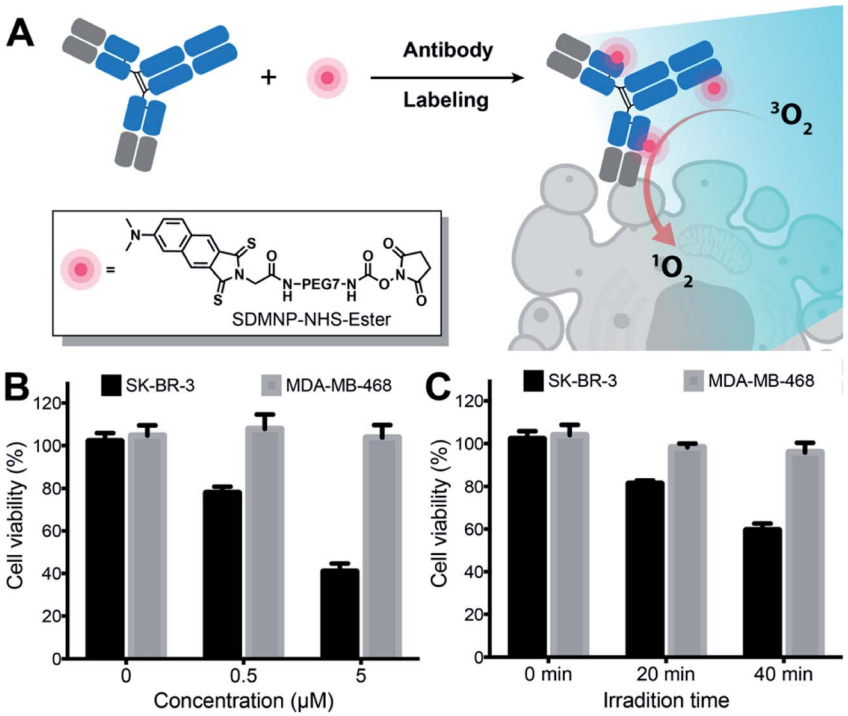

Fig. 4 (A) Scheme of the antibody-photosensitizer conjugate (Tras-SDMNP) for photoimmunotherapy. (B) Cytotoxicity assays performed with SK-BR-3 and MDA-MB-468 cells with different concentrations of Tras-SDMNP. (C) Cell viability of SK-BR-3 and MDA-MB-468 cells with 0.5 μM Tras-SDMNP after different irradiation times.

Conclusions

In summary, we have developed a general strategy for preparing visible/NIR light-absorbing, heavy-atom-free PSs by performing a simple sulfur-for-oxygen atom replacement within traditional fluorescent molecules. Starting with the parental carbonyl congeners, we used a simple one-pot-synthesis to prepare a set of thio-based PSs spanning a broad spectral range. We found that these thio-based PSs exhibited high singlet oxygen-generating abilities with near-unity singlet oxygen quantum yields. Theoretical calculations indicated that thiocarbonyl substitution resulted in significant increases in SOC constants compared to the parental carbonyl compounds, echoing the high singlet oxygen quantum yields of thio-based PSs. In addition to generating high singlet oxygen quantum yields, the sulfur-for-oxygen atom substitution within existing fluorophores also leads to a significant bathochromic shift of absorption maxima to red or NIR regions and to enhanced extinction coefficients, both of which will be important for improving tissue penetration during treatment of tumors. Our *in vitro* data demonstrate that thio-based PSs can exert robust photodynamic therapeutic effects on both monolayer cancer cells and 3D multicellular tumor spheroids following irradiation with white light, red light, or NIR light, and that these effects are mediated by photo-induced intracellular ROS. Furthermore, we have demonstrated the utility of these thio-based PSs for photoimmunotherapy by conjugation of SDMNP to trastuzumab, a monoclonal antibody directed against HER2. The conjugate exhibited robust cytotoxicity against a HER2-positive cell line but had little effect on HER2-negative cells. This type of strategy thus holds great promise for selectively treating HER2 positive breast cancers. Given the versatility of this strategy for designing PSs, we envision that these thio-based reagents are not limited to the usage in PDT but can also serve as diverse PSs in photocatalytic organic reactions, photovoltaics and triplet–triplet annihilation.

Conflicts of interest

There are no conflicts to declare.

Acknowledgements

This work was supported by the Cancer Prevention Research Institute of Texas (CPRIT RR170014), NIH (R35-GM133706), the Robert A. Welch Foundation (C-1970), the John S. Dunn Foundation Collaborative Research Award, and the Hamill Innovation Award. H. X. is a Cancer Prevention & Research Institute of Texas (CPRIT) Scholar in Cancer Research.

Notes and references

1 T. J. Dougherty, C. J. Gomer, B. W. Henderson, G. Jori, D. Kessel, M. Korbelik, J. Moan and Q. Peng, *J. Natl. Cancer Inst.*, 1998, **90**, 889–905.
2 I. J. Macdonald and T. J. Dougherty, *J. Porphyrins Phthalocyanines*, 2001, **05**, 105–129.

3 A. P. Castano, T. N. Demidova and M. R. Hamblin, *Photodiagn. Photodyn. Ther.*, 2004, **1**, 279–293.
4 R. R. Allison and K. Moghissi, *Clin. Endosc.*, 2013, **46**, 24–29.
5 K. Chang, Z. Liu, X. Fang, H. Chen, X. Men, Y. Yuan, K. Sun, X. Zhang, Z. Yuan and C. Wu, *Nano Lett.*, 2017, **17**, 4323–4329.
6 T. Nagaya, A. P. Gorka, R. R. Nani, S. Okuyama, F. Ogata, Y. Maruoka, P. L. Choyke, M. J. Schnermann and H. Kobayashi, *Mol. Cancer Ther.*, 2018, **17**, 661–670.
7 D. E. J. G. J. Dolmans, D. Fukumura and R. K. Jain, *Nat. Rev. Cancer*, 2003, **3**, 380–387.
8 S. B. Brown, E. A. Brown and I. Walker, *Lancet Oncol.*, 2004, **5**, 497–508.
9 A. P. Castano, P. Mroz and M. R. Hamblin, *Nat. Rev. Cancer*, 2006, **6**, 535–545.
10 J. F. Lovell, T. W. B. Liu, J. Chen and G. Zheng, *Chem. Rev.*, 2010, **110**, 2839–2857.
11 P. Agostinis, K. Berg, K. A. Cengel, T. H. Foster, A. W. Girotti, S. O. Gollnick, S. M. Hahn, M. R. Hamblin, A. Juzeniene, D. Kessel, M. Korbelik, J. Moan, P. Mroz, D. Nowis, J. Piette, B. C. Wilson and J. Golab, *CA: Cancer J. Clin.*, 2011, **61**, 250–281.
12 W. Fan, P. Huang and X. Chen, *Chem. Soc. Rev.*, 2016, **45**, 6488–6519.
13 M. Ochsner, *J. Photochem. Photobiol., B*, 1997, **39**, 1–18.
14 B. C. Wilson and M. S. Patterson, *Phys. Med. Biol.*, 2008, **53**, R61–R109.
15 K. Plaetzer, B. Krammer, J. Berlanda, F. Berr and T. Kiesslich, *Laser Med. Sci.*, 2009, **24**, 259–268.
16 S. Kolemen, M. Işık, G. M. Kim, D. Kim, H. Geng, M. Buyuktemiz, T. Karatas, X. F. Zhang, Y. Dede, J. Yoon and E. U. Akkaya, *Angew. Chem., Int. Ed. Engl.*, 2015, **54**, 5340–5344.
17 E. D. Anderson, A. P. Gorka and M. J. Schnermann, *Nat. Commun.*, 2016, **7**, 13378.
18 S. Callaghan and M. O. Senge, *Photochem. Photobiol. Sci.*, 2018, **17**, 1490–1514.
19 Y. Ning, Y.-W. Liu, Z.-S. Yang, Y. Yao, L. Kang, J. L. Sessler and J.-L. Zhang, *J. Am. Chem. Soc.*, 2020, **142**, 6761–6768.
20 J. R. Darwent, P. Douglas, A. Harriman, G. Porter and M.-C. Richoux, *Coord. Chem. Rev.*, 1982, **44**, 83–126.
21 R. R. Allison, G. H. Downie, R. Cuenca, X.-H. Hu, C. J. Childs and C. H. Sibata, *Photodiagn. Photodyn. Ther.*, 2004, **1**, 27–42.
22 Y. Cakmak, S. Kolemen, S. Duman, Y. Dede, Y. Dolen, B. Kilic, Z. Kostereli, L. T. Yildirim, A. L. Dogan, D. Guc and E. U. Akkaya, *Angew. Chem., Int. Ed. Engl.*, 2011, **50**, 11937–11941.
23 N. J. Patel, Y. Chen, P. Joshi, P. Pera, H. Baumann, J. R. Missert, K. Ohkubo, S. Fukuzumi, R. R. Nani, M. J. Schnermann, P. Chen, J. Zhu, K. M. Kadish and R. K. Pandey, *Bioconjugate Chem.*, 2016, **27**, 667–680.
24 L. Huang, X. Cui, B. Therrien and J. Zhao, *Chem.–Eur. J.*, 2013, **19**, 17472–17482.
25 J. Tang, J.-J. Chen, J. Jing, J.-Z. Chen, H. Lv, Y. Yu, P. Xu and J.-L. Zhang, *Chem. Sci.*, 2013, **5**, 558–566.
26 W. Wu, X. Cui and J. Zhao, *Chem. Commun.*, 2013, **49**, 9009–9011.
27 J. Zhao, W. Wu, J. Sun and S. Guo, *Chem. Soc. Rev.*, 2013, **42**, 5323–5351.
28 J. Peng, X. Guo, X. Jiang, D. Zhao and Y. Ma, *Chem. Sci.*, 2016, **7**, 1233–1237.
29 L. Zhang, Z. Huang, D. Dai, Y. Xiao, K. Lei, S. Tan, J. Cheng, Y. Xu, J. Liu and X. Qian, *Org. Lett.*, 2016, **18**, 5664–5667.
30 M. A. Filatov, S. Karuthedath, P. M. Polestshuk, S. Callaghan, K. J. Flanagan, M. Telitchko, T. Wiesner, F. Laquai and M. O. Senge, *Phys. Chem. Chem. Phys.*, 2018, **20**, 8016–8031.
31 M. A. Filatov, *Org. Biomol. Chem.*, 2019, **18**, 10–27.
32 A. Massey, Y. Z. Xu and P. Karran, *Curr. Biol.*, 2001, **11**, 1142–1146.
33 O. Reelfs, Y.-Z. Xu, A. Massey, P. Karran and A. Storey, *Mol. Cancer Ther.*, 2007, **6**, 2487–2495.
34 P. Karran and N. Attard, *Nat. Rev. Cancer*, 2008, **8**, 24–36.
35 L. Martínez-Fernández, I. Corral, G. Granucci and M. Persico, *Chem. Sci.*, 2014, **5**, 1336–1347.
36 M. Pollum, S. Jockusch and C. E. Crespo-Hernández, *J. Am. Chem. Soc.*, 2014, **136**, 17930–17933.
37 J. D. Coyle, *Tetrahedron*, 1985, **41**, 5393–5425.
38 A. Maciejewski and R. P. Steer, *Chem. Rev.*, 1993, **93**, 67–98.
39 S. Mai, M. Pollum, L. Martínez-Fernández, N. Dunn, P. Marquetand, I. Corral, C. E. Crespo-Hernández and L. González, *Nat. Commun.*, 2016, **7**, 13077.
40 K. M. Farrell, M. M. Brister, M. Pittelkow, T. I. Sølling and C. E. Crespo-Hernández, *J. Am. Chem. Soc.*, 2018, **140**, 11214–11218.
41 B. Ashwood, M. Pollum and C. E. Crespo-Hernández, *Photochem. Photobiol.*, 2019, **95**, 33–58.
42 J. Tang, M. A. Robichaux, K.-L. Wu, J. Pei, N. T. Nguyen, Y. Zhou, T. G. Wensel and H. Xiao, *J. Am. Chem. Soc.*, 2019, **141**, 14699–14706.
43 V.-N. Nguyen, S. Qi, S. Kim, N. Kwon, G. Kim, Y. Yim, S. Park and J. Yoon, *J. Am. Chem. Soc.*, 2019, **141**, 16243–16248.
44 W. Spiller, H. Kliesch, D. Wöhrle, S. Hackbarth, B. Röder and G. Schnurpfeil, *J. Porphyrins Phthalocyanines*, 1998, **2**, 145–158.
45 Z. Lv, H. Wei, Q. Li, X. Su, S. Liu, K. Y. Zhang, W. Lv, Q. Zhao, X. Li and W. Huang, *Chem. Sci.*, 2018, **9**, 502–512.
46 W. Li, L. Li, H. Xiao, R. Qi, Y. Huang, Z. Xie, X. Jing and H. Zhang, *RSC Adv.*, 2013, **3**, 13417–13421.
47 R.-Z. Lin, R.-Z. Lin and H.-Y. Chang, *Biotechnol. J.*, 2008, **3**, 1172–1184.
48 F. Hirschhaeuser, H. Menne, C. Dittfeld, J. West, W. Mueller-Klieser and L. A. Kunz-Schughart, *J. Biotechnol.*, 2010, **148**, 3–15.
49 G. Lazzari, P. Couvreur and S. Mura, *Polym. Chem.*, 2017, **8**, 4947–4969.
50 L. A. Kunz-Schughart, M. Kreutz and R. Knuechel, *Int. J. Exp. Pathol.*, 1998, **79**, 1–23.
51 M. T. Santini and G. Rainaldi, *Pathobiol. J. Immunopathol. Mol. Cell Biol.*, 1999, **67**, 148–157.
52 J. Friedrich, C. Seidel, R. Ebner and L. A. Kunz-Schughart, *Nat. Protoc.*, 2009, **4**, 309–324.
53 L. Mohammad-Hadi, A. J. MacRobert, M. Loizidou and E. Yaghini, *Nanoscale*, 2018, **10**, 1570–1581.

54 M. Mitsunaga, M. Ogawa, N. Kosaka, L. T. Rosenblum, P. L. Choyke and H. Kobayashi, *Nat. Med.*, 2011, **17**, 1685–1691.
55 J. P. Tardivo, A. Del Giglio, C. S. de Oliveira, D. S. Gabrielli, H. C. Junqueira, D. B. Tada, D. Severino, R. de Fátima Turchiello and M. S. Baptista, *Photodiagn. Photodyn. Ther.*, 2005, **2**, 175–191.
56 W. Jakubowski and G. Bartosz, *Cell Biol. Int.*, 2000, **24**, 757–760.
57 X.-S. Ke, J. Tang, J. Chen, Z. Zhou and J.-L. zhang, *ChemPlusChem*, 2015, **80**, 237–252.
58 M. Y. Li, C. S. Cline, E. B. Koker, H. H. Carmichael, C. F. Chignell and P. Bilski, *Photochem. Photobiol.*, 2001, **74**, 760–764.
59 M. Bancirova, *J. Biol. Chem. Lumin.*, 2011, **26**, 685–688.
60 F. De Vita, F. Giuliani, N. Silvestris, G. Catalano, F. Ciardiello and M. Orditura, *Canc. Treat. Rev.*, 2010, **36**, S11–S15.
61 J. Mathew and E. A. Perez, *Curr. Opin. Oncol.*, 2011, **23**, 594–600.
62 N. Iqbal and N. Iqbal, *Human Epidermal Growth Factor Receptor 2 (HER2) in Cancers*, https://www.hindawi.com/journals/mbi/2014/852748/, accessed April 3, 2020.

